University of Baghdad
College of Engineering
JOURNAL OF ENGINEERING

Journal of Engineering

journal homepage: www.jcoeng.edu.iq

Volume 31 Number 3 March 2025

Design of an Optimal SMC Controller for a Twin Rotor Aerodynamic System

Marwa Rasheed Ali *, **Omer Waleed Abdulwahhab**

Department of Computer Engineering, College of Engineering, University of Baghdad, Baghdad, Iraq

ABSTRACT

This paper presents a multi-input multi-output (MIMO) high-coupled nonlinear model of a twin-rotor aerodynamic system (TRAS). An optimal sliding mode controller (SMC) is proposed to control the TRAS system. Two optimization algorithms, namely Grey Wolf Optimization (GWO) and Whale Optimization Algorithm (WOA), are used to tune the SMC's parameters. Which are effectively implemented in this controller. The simulation results are given to demonstrate its effectiveness. To evaluate the performance of the proposed controller, a comparison with a previous study—that used Genetic Algorithm (GA), Particle Swarm Optimization (PSO), and Simulated Annealing (SA) algorithms—has been conducted. The results of the proposed controller reveal better performance indices than the previous study. In addition, a novel performance index is presented in this paper as an objective function for designing SMC parameters. Which is identified by the Integral of Quadric Time multiplied by Absolute Error (IQTAE). To verify the effectiveness of the proposed IQTAE, a comparison was conducted with the previous study that used traditional performance indices (ISE, IAE, ITSE, ITAE). To guarantee a fair comparison, apply the same optimization algorithms (GA), (PSO), and (SA) that were utilized in the previous study. By using this method, it was possible to compare the performance indices under the same conditions. The simulation results show the superiority of the novel performance index, especially in reducing overshoot. The percentage enhancements of the overshoot of both azimuth and pitch angles reach, respectively, 58.7% and 99.35% with GA, -0.65% and 70.1% with PSO, and 44.53% and 88.59% with SA.

Keywords: SMC controller, TRAS, Twin rotor aerodynamic system, Frequency response specifications.

1. INTRODUCTION

The Twin twin-rotor aerodynamic System (TRAS) is an experimental device that mimics the behavior of a helicopter. The TRAS has gained a lot of interest because there are similarities between the dynamics of a helicopter and the TRAS in certain aspects **(Wen and Lu, 2008;**

*Corresponding author
Peer review under the responsibility of University of Baghdad.
https://doi.org/10.31026/j.eng.2025.03.03

Article received: 08/06/2024
Article revised: 08/09/2024
Article accepted: 21/11/2024
Article published: 01/03/2025

Tao et al., 2010). Several researchers decided to go for the twin rotor multi-input multi-output system (MIMO) as a laboratory prototype model due to the high cost of the helicopter system model **(Jagadeb et al., 2021)**. The basic element of the TRAS system is a beam that supports two rotors, the tail rotor, and the main rotor, that propel the helicopter in different directions along the horizontal (azimuth) and vertical (pitch) angles. Two DC motors are used to power these rotors. The TRAS system has two outputs, which are the angles of the two rotors, and two inputs, which are the applied voltage of the two DC motors **(Bayrak et al., 2015; Roman et al., 2018; Faris et al., 2017)**.

Since the TRAS is a MIMO nonlinear system with high nonlinearity and a strong cross-coupling relationship between its two channels, controlling this system has become one of the most difficult engineering issues to solve **(Abdulwahhab and Abbas, 2020)**. When modeling the TRAS, several assumptions and simplifications have been proposed, which results in a model uncertainty issue, so creating accurate models for nonlinear plants is almost impossible **(Rahideh et al., 2008; Tee et al., 2008; Butt and Aschemann, 2015)**. Even if we obtain a system model, it may not accurately reflect the real system **(Wen and Li, 2011).** The control goal is to make the TRAS beam move to trace a trajectory or arrive at predetermined points in two degrees of freedom. It also aims to stabilize the system when it is in a coupled state. Different techniques have been devised to control this system. The proportional-integral-differential (PID) is the most commonly used controller in the industry due to its straightforward design and simplicity of implementation **(Apkarian et al., 2007; Almtireen et al., 2018; Mihaly et al., 2021).** Many studies have been carried out to tune the PID parameters **(Borase et al., 2021)**.

(Pandey and Laxmi, 2014) have developed a PID controller with a derivative filter coefficient. The outcomes of the simulation and the traditional PID controller are contrasted. The suggested PlD controller with a derivative filter exhibits superior transient and steady-state responsiveness. However, the drawback of the PID controller is that it is less intelligent since its parameters are partially adjusted by trial and error **(Juang et al., 2011)**. Therefore, to increase performance for the TRAS, PID is frequently enhanced with additional control algorithms. In **(Liu et al., 2011)**, fuzzy logic has been used with the PID control. The outcomes demonstrate the success of the suggested approach in obtaining favorable outcomes in both directions of motion. Ref**. (Faisal and Abdulwahhab, 2021a)** suggest a hybrid design process that merges root locus and frequency response methodologies called PID-Lead Compensator (PIDLC). The PIDLC operates better than the PID controller because the response oscillation was removed and the system's relative stability was raised. Although controller augmentation can improve performance, it causes the system's response time to increase. In **(Faisal and Abdulwahhab, 2021b)**, a control strategy based on applying a Linear Quadratic Regulator (LQR) and Adaptive Linear Quadratic Regulator (ALQR) for TRAS stabilization has been used. When designing the controller, the TRAS system's uncertainties should be considered because they significantly affect the controller's performance. To overcome this issue and to achieve robust behavior against modeling uncertainty and external disturbances, a robust H∞ controller is used **(Paul and Jacob, 2020; Jagadeb et al., 2021)**. The limitation of the H∞ controller is that it requires linearization of the nonlinear TRAS **(Kumar and Hote, 2021).** There are different kinds of fractional order controllers used to control the TRAS. In **(Abdulwahhab and Abbas, 2017)**, a FOPID has been designed. The simulation results showed that the FOPID controller enhanced all performance indices compared to the integer-order equivalent PID controller and was more robust against changes in the TRAS parameters.

However, all previous controllers used are linear and need to linearize the TRAS. There is a drawback to using the linearization design approach for highly nonlinear systems, like the TRAS **(Faisal and Abdulwahhab, 2021a).** Thus, a nonlinear robust finite-time SMC to manage the TRAS system **(Choudhary and Muthukumar, 2020)**. This controller uses a finite-time SMC approach for achieving the required trajectory or position stability. Numerical simulation results prove the efficiency of the control strategy. **(Palepogu and Mahapatra, 2024)** proposed a sliding mode control with state-varying gains (VGSMC) technique for the horizontal plane of the TRAS system. The robustness of this controller is tested by adding white noise as uncertainty to the TRAS system. The VGSMC controller is designed to eliminate chattering without compromising robustness features, as well as to reduce the overestimation of control effort. A comparison of the twisting algorithm (TA) and VGSMC is done to highlight the benefits of the designed control technique. The conclusion is that VGSMC can overcome the TA controller's limitation, which is the chattering effect, and the traditional SMC limitation, which is the energy consumption.
The objective of this study is to design an optimal SMC controller using GWO and WOA for the TRAS system. To analyze the performance of the proposed controller, a comparison with a previous study that adopted (GA, PSO, and SA) algorithms has been carried out. Also, a novel performance index is presented in this paper called the Integral of Quadric Time multiplied by Absolute Error (IQTAE) which serves as an objective function for tuning the SMC parameters. The IQTAE enhances the performance of the controller by reducing the overshoot compared to the previous study.

2. MATHEMATICAL MODEL OF THE TRAS

The mechanical structure of the TRAS is made up of two rotors mounted on a beam, as shown in the schematic diagram of the twin rotor in **Fig. 1**.

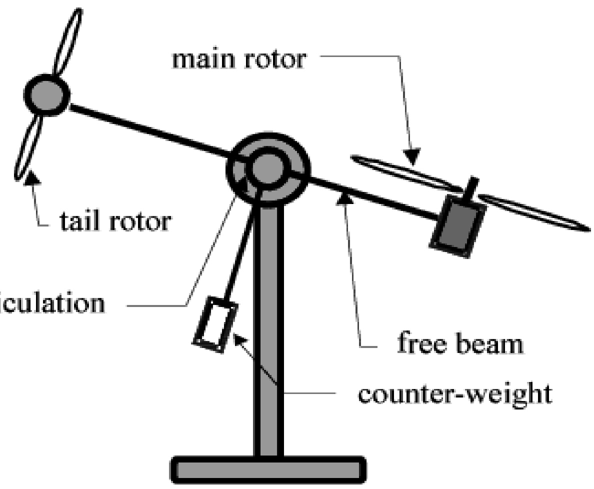

Figure 1. Schematic diagram of TRAS system.

The differential equations that reflect the TRAS's dynamics are derived using Lagrange's equations **(Abdulwahhab and Abbas, 2017)**. The dynamics of this system are represented by the nonlinear equations.

$$J_{\phi}\ddot{\phi} = F_t(\omega_t)l_t cos\theta - \left(c_{\phi}\dot{\phi} + k_{\phi}\phi\right) + J\dot{\phi}\dot{\theta}\, sin\,(2\theta) \quad (1)$$

$$J_\theta \ddot{\theta} = F_m(\omega_m) l_m - (c_\theta \dot{\theta} + k_\theta \theta) - (k_1 \cos\theta + k_2 \sin\theta) - J \frac{\dot{\phi}^2}{2} \sin(2\theta) \quad (2)$$

where the parameters of the TRAS system are shown in **Table 1**, and the angular velocities of the tail and main rotors are

$$\dot{\omega}_t = -\frac{1}{T_t}\omega_t + \frac{g_t}{T_t}u_t \quad (3)$$

$$\dot{\omega}_m = -\frac{1}{T_m}\omega_m + \frac{g_m}{T_m}u_m \quad (4)$$

Where ϕ and θ are the azimuth and pitch angles of the tail and main rotors, respectively; and u_t and u_m are the input voltages that are applied to the tail and main DC motors, respectively. So, Eq. (1) and Eq. (3) represent the dynamics of the tail horizontal subsystem, and Eq. (2) and Eq. (4) represent the dynamics of the main vertical subsystem.

Strong cross-coupling exists between the dynamics of the main rotor and tail rotor in TRAS (the last term in both Eq. (1) and Eq. (2)), in addition to the first term in Eq. (1).

The variables $\boldsymbol{J_\phi}$ and $\boldsymbol{J_\theta}$ depict the sums of moments of inertia for the horizontal and vertical axes, respectively, which are

$$J_\phi = m_m l_m^2 \cos^2\theta + m_t l_t^2 \cos^2\theta + 2 m_{cw} l_{cw}^2 \sin^2\theta = J\cos^2\theta + J_A$$

$$J_A = m_{cw} l_{cw}^2$$

$$J = m_m l_m^2 + m_t l_t^2 - m_{cw} l_{cw}^2$$

$$J_\theta = m_m l_m^2 + m_t l_t^2 + m_{cw} l_{cw}^2$$

$$k_1 = g(m_m l_m - m_t l_t)$$

$$k_2 = g m_{cw} l_{cw}$$

where

l_t the tail portion of the beam's length.
l_m the main portion of the beam's length.
k_ϕ the torque restoration coefficient in the horizontal plane.
k_θ the torque restoration coefficient in the vertical plane.
c_ϕ the horizontal plane's velocity-proportional friction torque coefficient.
c_θ the vertical plane's velocity-proportional friction torque coefficient.
k_1 the first coefficient concerning the horizontal plane.
k_2 the second coefficient for the horizontal plane.
g_t the tail rotor's DC gain.
g_m the main rotor's DC gain.
T_t the tail rotor's time constant.
T_m the main rotor's time constant.
l_{cw} the length of a counterweight rod with a point mass attached to the end of it.
$m_m$the main propeller's mass.
m_t the tail propeller's mass.
m_{cw} the Point masses connected to the ends of the counterweight rods.
g the acceleration due to gravity.

The relationships between the main rotor's and tail rotor's propulsive forces and angular velocities are as follows:

$$F_t(\omega_t) = -3\times10^{-14}\omega_t^5 - 1.595\times10^{-11}\omega_t^4 + 2.511\times10^{-7}\omega_t^3 - 1.808\times10^{-4}\omega_t^2 + 0.801\omega_t \quad (5)$$

$$F_m(\omega_m) = -3.48\times10^{-12}\omega_m^5 + 1.09\times10^{-9}\omega_m^4 + 4.12310^{-6}\omega_m^3 - 1.632\times10^{-4}\omega_m^2 + 9.544\times10^{-2}w \quad (6)$$

Table 1. Parameters of the TRAS system.

Parameter	Value
J_A	$0.0561\ kg.m^2$
J_θ	$0.0559\ kg.m^2$
T_m	$2.5\ s$
T_t	$5\ s$
c_θ	$0.0100\ N.m.s$
c_ϕ	$0.0100\ N.m.s$
g_m	22.7273
g_t	18.1818
k_1	$5.00576\times10^{-2}\ N.m$
k_2	$9.36008\times10^{-2} N.m$
k_θ	$0.0600\ N.m$
k_ϕ	$0.0600\ N.m$
l_m	$0.2400\ m$
l_t	$0.2500\ m$
m_{cw}	$0.068\ kg$
m_m	$0.0145\ kg$
m_t	$0.0155\ kg$
J	$0.2168\ kg.m^2$

A state-space model of the TRAS is $\dot{x} = f(x,u)$ and it is:

$$\dot{\boldsymbol{x}} = \begin{bmatrix} x_2 \\ \frac{1}{J\cos^2 x_4 + J_A}\left(F_t(x_3)l_t\cos x_4 - c_\phi x_2 - k_\phi x_1 + Jx_2x_5\sin 2x_4\right) \\ -\frac{1}{T_t}x_3 + \frac{g_t}{T_t}u_t \\ x_5 \\ \frac{1}{J_\theta}\left(F_m(x_6)l_m - k_1\cos x_4 - k_2\sin x_4 - \frac{J}{2}x_2^2\sin 2x_4 - c_\theta x_5 - k_\theta x_4\right) \\ -\frac{1}{T_m}x_6 + \frac{g_m}{T_m}u_m \end{bmatrix} \quad (7)$$

$$\boldsymbol{y} = \begin{bmatrix} 1\ 0\ 0\ 0\ 0\ 0 \\ 0\ 0\ 0\ 1\ 0\ 0 \end{bmatrix}\boldsymbol{x} \quad (8)$$

where

$x = [\phi, \dot{\phi}, \omega_t, \theta, \dot{\theta}, \omega_m]^T$ the state vector, $u = [u_t\ u_m]^T$ the input vector, and $y = [\phi\ \theta]^T$ the output vector.

3. SLIDING MODE CONTROLLER

Sliding mode control is a nonlinear control technique that produces robust control systems by rejecting disturbances and being insensitive to parameter variations **(Allouani et al., 2012; Hamoudi, 2016; Rashad et al., 2017)**. Two SMCs are needed to control the TRAS, one for the horizontal subsystem and the other for the vertical subsystem. The cross-coupling effect between the two channels is considered a disturbance input to each subsystem **(Mishra et al., 2019)**.

3.1 Design of Sliding Mode Controller for a Horizontal Subsystem

The sliding surface of the horizontal subsystem is

$$s_\phi = a_\phi x_2 + b_\phi x_1 + x_3 \tag{9}$$

$$\dot{s}_\phi = a_\phi \dot{x}_2 + b_\phi \dot{x}_1 + \dot{x}_3$$

$$\dot{s}_\phi = \frac{a_\phi}{J cos^2(x_4)+J_A}\left(F_t(x_3) l_t cos\, x_4 - c_\phi x_2 - k_\phi x_1 + J x_2 x_5 \sin 2x_4\right) + b_\phi x_2 - \frac{1}{T_t} x_3 + \frac{g_t}{T_t} u_t \tag{10}$$

$$\dot{s}_\phi = 0 \implies$$

$$u_{t\_eq} = \frac{T_t}{g_t}\left(\frac{-a_\phi}{J cos^2(x_4)+J_A}\left(F_t(x_3) l_t cos\, x_4 - c_\phi x_2 - k_\phi x_1 + J x_2 x_5 \sin 2x_4\right) - b_\phi x_2 + \frac{1}{T_t} x_3\right) \tag{11}$$

$$u_t = u_{t\_eq} - \beta_\phi \mathrm{sgn}(s_\phi) \implies$$

$$u_t = \frac{T_t}{g_t}\left(\frac{-a_\phi}{J cos^2(x_4)+J_A}\left(F_t(x_3) l_t cos\, x_4 - c_\phi x_2 - k_\phi x_1 + J x_2 x_5 \sin 2x_4\right) - b_\phi x_2 + \frac{1}{T_t} x_3\right) - \beta_\phi \mathrm{sgn}(s_\phi) \tag{12}$$

Reaching Phase of the Horizontal Subsystem of SMC

To demonstrate that the trajectory of the horizontal subsystem arrives at the horizontal sliding surface in a finite time, let

$$W = |s_\phi|$$

$$\frac{dW}{dt} = \mathrm{sgn}(s_\phi)\dot{s}_\phi$$

Eq. (12) is substituted in Eq. (10) to produce

$$\dot{s}_\phi = \frac{a_\phi}{J cos^2(x_4)+J_A}\left(F_t(x_3) l_t cos\, x_4 - c_\phi x_2 - k_\phi x_1 + J x_2 x_5 \sin 2x_4\right) + b_\phi x_2 - \frac{1}{T_t} x_3 + \frac{g_t}{T_t}\left(\frac{T_t}{g_t}\left(\frac{-a_\phi}{J cos^2(x_4)+J_A}\left(F_t(x_3) l_t cos\, x_4 - c_\phi x_2 - k_\phi x_1 + J x_2 x_5 \sin 2x_4\right) - b_\phi x_2 + \frac{1}{T_t} x_3\right) - \beta_\phi sgn(s_\phi)\right)$$

$$\dot{s}_\phi = -\frac{g_t}{T_t}\beta_\phi \mathrm{sgn}(s_\phi)$$

$$\frac{dW}{dt} = sgn(s_\phi)\left(-\frac{g_t}{T_t}\beta_\phi sgn(s_\phi)\right) = -\frac{g_t}{T_t}\beta_\phi$$

$$\frac{d|s_\phi|}{d\tau} = -\frac{g_t}{T_t}\beta_\phi \tag{13}$$

Integrating both sides of Eq. (13) concerning τ from 0 to t yields:

$$\left|s_\phi\right|\Big]_0^t = -\frac{g_t}{T_t}\beta_\phi\tau\Big]_0^t$$

$$\left|s_\phi(t)\right| - \left|s_\phi(0)\right| = -\frac{g_t}{T_t}\beta_\phi t$$

$$\left|s_\phi(t_s)\right| - \left|s_\phi(0)\right| = -\frac{g_t}{T_t}\beta_\phi t_{s\phi}$$

At $t = t_s,\ s_\phi(t_{s\phi}) = 0$

$$0 - \left|s_\phi(0)\right| = -\frac{g_t}{T_t}\beta_\phi t_{s\phi}$$

$$t_{s\phi} = \frac{\left|s_\phi(0)\right|}{\frac{g_t}{T_t}\beta_\phi} \tag{14}$$

3.2 Design of Sliding Mode Controller for a Vertical Subsystem

The sliding surface of the vertical subsystem is

$$s_\theta = a_\theta x_5 + b_\theta x_4 + x_6$$

$$\dot{s}_\theta = a_\theta \dot{x}_5 + b_\theta \dot{x}_4 + \dot{x}_6 \tag{15}$$

$$\dot{s}_\theta = \frac{a_\theta}{J_\theta}\left(F_m(x_6)l_m - k_1\cos x_4 - k_2\sin x_4 - \frac{J}{2}x_2^2\sin 2x_4 - c_\theta x_5 - k_\theta x_4\right) + b_\theta x_5 - \frac{1}{T_m}x_6 + \frac{g_m}{T_m}u_m \tag{16}$$

$\dot{s}_\theta = 0 \quad \Longrightarrow$

$$u_{m\_eq} = \frac{T_m}{g_m}\left(\frac{-a_\theta}{J_\theta}\left(F_m(x_6)l_m - k_1\cos x_4 - k_2\sin x_4 - \frac{J}{2}x_2^2\sin x_4\sin 2x_4 - c_\theta x_5 - k_\theta x_4\right) - b_\theta x_5 + \frac{1}{T_m}x_6\right. \tag{17}$$

$u_m = u_{m\_eq} - \beta_\theta \operatorname{sgn}(s_\theta) \Longrightarrow$

$$u_m = \frac{T_m}{g_m}\left(\frac{-a_\theta}{J_\theta}\left(F_m(x_6)l_m - k_1\cos x_4 - k_2\sin x_4 - \frac{J}{2}x_2^2\sin x_4\sin 2x_4 - c_\theta x_5 - k_\theta x_4\right) - b_\theta x_5 + \frac{1}{T_m}x_6 - \beta_\theta \operatorname{sgn}(s_\theta)\right. \tag{18}$$

Reaching Phase of the Vertical Subsystem of SMC

To demonstrate that the trajectory of the horizontal subsystem arrives at the vertical sliding surface in a finite time, let

$$W = |s_\theta|$$

$$\frac{dW}{dt} = \operatorname{sgn}(s_\theta)\dot{s}_\theta$$

Eq. (18) is substituted in Eq. (16) to produce

$$\dot{s}_\theta = \frac{a_\theta}{J_\theta}\left(F_m(x_6)l_m - k_1\cos x_4 - k_2\sin x_4 - \frac{J}{2}x_2^2\sin 2x_4 - c_\theta x_5 - k_\theta x_4\right) + b_\theta x_5 - \frac{1}{T_m}x_6 + \frac{g_m}{T_m}\left(\frac{T_m}{g_m}\left(\frac{-a_\theta}{J_\theta}\left(F_m(x_6)l_m - k_1\cos x_4 - k_2\sin x_4 - \frac{J}{2}x_2^2\sin x_4\sin 2x_4 - c_\theta x_5 - k_\theta x_4\right) - b_\theta x_5 + \frac{1}{T_m}x_6 - \beta_\theta \operatorname{sgn}(s_\theta)\right)\right.$$

$\dot{s}_\theta = -\frac{g_\mathrm{m}}{T_\mathrm{m}}\beta_\theta \mathrm{sgn}(s_\theta)$

$\frac{dW}{dt} = \mathrm{sgn}(s_\theta)\left(-\frac{g_\mathrm{m}}{T_\mathrm{m}}\beta_\phi \mathrm{sgn}(s_\theta)\right) = -\frac{g_\mathrm{m}}{T_\mathrm{m}}\beta_\theta$

$$\frac{d|s_\theta|}{d\tau} = -\frac{g_\mathrm{m}}{T_\mathrm{m}}\beta_\theta \tag{19}$$

Integrating both sides of Eq. (19) with respect to τ from 0 to t yields:

$|s_\theta|]_0^t = -\frac{g_\mathrm{m}}{T_\mathrm{m}}\beta_\theta \tau\Big]_0^t$

$|s_\theta(t)| - |s_\theta(0)| = -\frac{g_\mathrm{m}}{T_\mathrm{m}}\beta_\theta t$

$|s_\theta(t_{s\theta})| - |s_\theta(0)| = -\frac{g_\mathrm{m}}{T_\mathrm{m}}\beta_\theta t_{s\theta}$

At $t = t_{s\theta}$, $s_\theta(t_{s\theta}) = 0$

$0 - |s_\theta(0)| = -\frac{g_\mathrm{m}}{T_\mathrm{m}}\beta_\theta t_{s\theta}$

$$t_{s\theta} = \frac{|s_\theta(0)|}{\frac{g_\mathrm{m}}{T_\mathrm{m}}\beta_\theta} \tag{20}$$

In Eq. (14) and Eq. (20), the time to reach the sliding surface t_{sj} $(j = \phi, \theta)$ is affected by the value of the parameter β_j. The amplitude of chattering increases, and t_{sj} decreases when β_j increases.

3.3 The Optimization Problem in Sliding Mode Controller

Dynamical systems often involve controllers with optimizing parameters to achieve the desired performance **(Chen et al., 2019)**. Optimization algorithms help to tune the controller coefficients. The SMC design vector can be formulated as an optimization problem, and the performance indices are determined as objective functions to be minimized. It is difficult to find a suitable optimization algorithm for every problem. The suitability of an algorithm depends on the specific problem, constraints, required performance criteria, and desired objectives. While algorithms succeed in solving one problem, they may not be efficient for other problems. Meta-heuristic optimization algorithms have gained a lot of popularity over the last few years **(Gao and Zhao, 2019)**. GWO is a swarm-based meta-heuristic algorithm. MirJalili invented this optimization algorithm in 2014, imitating the way of hunting and searching for grey wolves **(MirJalili et al., 2014)**. It has been proven to be more efficient than particle swarm optimization (PSO) and other bionic algorithms. GWO converges more quickly, has a high avoidance of local optima, and is easier to use compared to PSO **(Gao and Zhao, 2019)**. The WOA was tested on many problems and benchmarked with a well-known optimization algorithm. The comparison demonstrates competitive results against the most recent algorithms **(MirJalili and Lewis, 2016)**.

4. OPTIMAL SLIDING MODE CONTROLLER WITH FOUR PARAMETERS (SMC-4)

In order to design an optimal SMC-4, the sliding variable design parameters of the vertical and horizontal surface equations (Eq. (9) and Eq. (15)) are designed such that the system is stable while the state remains on the sliding surface; therefore, the design vector is $K_{SMC-4} = (a_\phi, b_\phi, a_\theta, b_\theta)$. In SMC-4, the values of β_θ and β_ϕ are set equal to 1 by trial and error. Two optimization algorithms, GWO and WOA are used to design the parameters of the SMC-4. The performance indices that are used as objective functions are

$$\text{ISE} = \int_0^\infty (0.5\, e_\phi(t)^2 + 0.5\, e_\theta(t)^2) dt$$
$$\text{IAE} = \int_0^\infty (0.5|e_\phi(t)| + 0.5|e_\theta(t)|) dt$$
$$\text{ITSE} = \int_0^\infty t(0.5\, e_\phi(t)^2 + 0.5\, e_\theta(t)^2) dt \quad (21)$$
$$\text{ITAE} = \int_0^\infty t(0.5|e_\phi(t)| + 0.5|e_\theta(t)|) dt$$

Where $e_\phi(t)$ is the error between the reference azimuth angle $\phi_r(t)$ and its actual value $\phi(t)$, and $e_\theta(t)$ is the error between the reference pitch angle $\theta_r(t)$ and its actual value $\theta(t)$.The reference values $\phi_r(t)$ and $\theta_r(t)$ are set equal to 1 rad and 0.1 rad, respectively, and the upper limit of the integration is set equal to 10 s.
Table 2 lists the SMC's designed parameters using the GWO and WOA optimization algorithms. By comparing the performance indices of this study with the previous study **(Faisal and Abdulwahhab, 2021c)** it is evident that the GWO optimization algorithm provides certain enhancements in all performance indices, indicating better overall error minimizing.

Table 2. Design parameters of SMC-4 using the GWO and WOA optimization algorithms.

parameters	IAE		ISE		ITAE		ITSE	
	GWO	WOA	GWO	WOA	GWO	WOA	GWO	WOA
a_ϕ	0.9277	1.3899	0.7802	1.5317	0.8450	0.7541	0.7848	0.7578
b_ϕ	5.1646	3.0188	4.8239	1.7427	5.2741	5.4559	5.0106	4.8669
a_θ	2.7073	3.6119	1.5873	1.4961	3.6236	3.8512	2.0724	2.2790
b_θ	0.2458	1.5879	0.0007	0.1075	1.1483	1.9344	0.0049	0.3412
Performance index	1.1883	1.2166	0.8623	0.8629	0.9529	0.9538	0.5233	0.5246

5. THE PROPOSED PERFORMANCE INDEX

In many applications, overshoot has negative effects like instability and mechanical harm, so a new performance index, designated by the Integral of Quadric Time multiplied by Absolute Error (IQTAE), is suggested as objective function to tune the SMC parameters. Which is defined by

$$\text{IQTAE}= \int_0^\infty t^4(0.5|e_\phi(t)| + 0.5|e_\theta(t)|)dt) \quad (22)$$

Also, the reference angles $\phi_r(t)$ and $\theta_r(t)$ are set to 1 rad and 0.1 rad, respectively, and the upper limit of the integration is set equal to 10 s. Table 3 shows the designed parameters of the SMC controller using the optimization algorithms (GA, PSO, and SA) and the IQTAE performance index. To verify the effectiveness of the proposed IQTAE, a comparison was conducted with the previous study that used traditional performance indices (ISE, IAE, ITSE, and ITAE).

Table 3. Design parameters of the performance index (IQTAE) of the SMC-4 system.

parameters	GA	PSO	SA
a_ϕ	1.9122	1.8346	1.9798
b_ϕ	3.2377	4.1105	4.8014
a_θ	8.2992	6.6257	7.5501
b_θ	1.1476	4.1793	3.5056
IQTAE	3.8468	4.0991	3.9729

To guarantee a fair comparison, apply the same optimization algorithms (GA), (PSO), and (SA) that were utilized in the previous study. By using this method, it was possible to compare the performance indices under the same conditions in an accurate manner.

6. SIMULATION RESULTS AND DISCUSSION

A simulation for the closed-loop system of the TRAS was carried out using MATLAB/R2020a for a simulation time of 10 s, as shown in **Figs. 2 to 9**, where the SMC-4 controller was implemented to the nonlinear coupled TRAS system. It is noticed from the system's response that the output of the tail rotor and the main rotor can follow the reference angles.
The simulation was based on the design vectors in Table 2, and by using these optimal parameters obtained by the two optimization algorithms (GWO and WOA), the simulation was carried out. The reference inputs for the TRAS are $(\phi_r, \theta_r) = (1, 0.1)$ rad and the initial position is chosen to be at $(\phi, \theta) = (0, -0.7098)$ rad. The time domain transient response specifications, the amplitude of chattering, the time to reach the sliding surface, and the performance indices (IAE, ISE, ITAE, and ITSE) values for SMC-4 are listed in **Tables 4 to 7**. The performance indices, which are grayscale-shaded, serve as the objective function utilized in the design vectors of the SMC-4. A comparison between the transient response specifications of this paper and the specifications obtained by the previous study **(Faisal and Abdulwahhab, 2021c)** was conducted. In this work, the outcomes are quite similar to the previous study, despite employing distinct algorithms, indicating that the approach and methodology applied have been validated. However, an alternative approach will be developed by employing a new performance index (IQTAE) to enhance performance and produce better results. It is expected that this approach will improve the outcomes and develop the field of study.

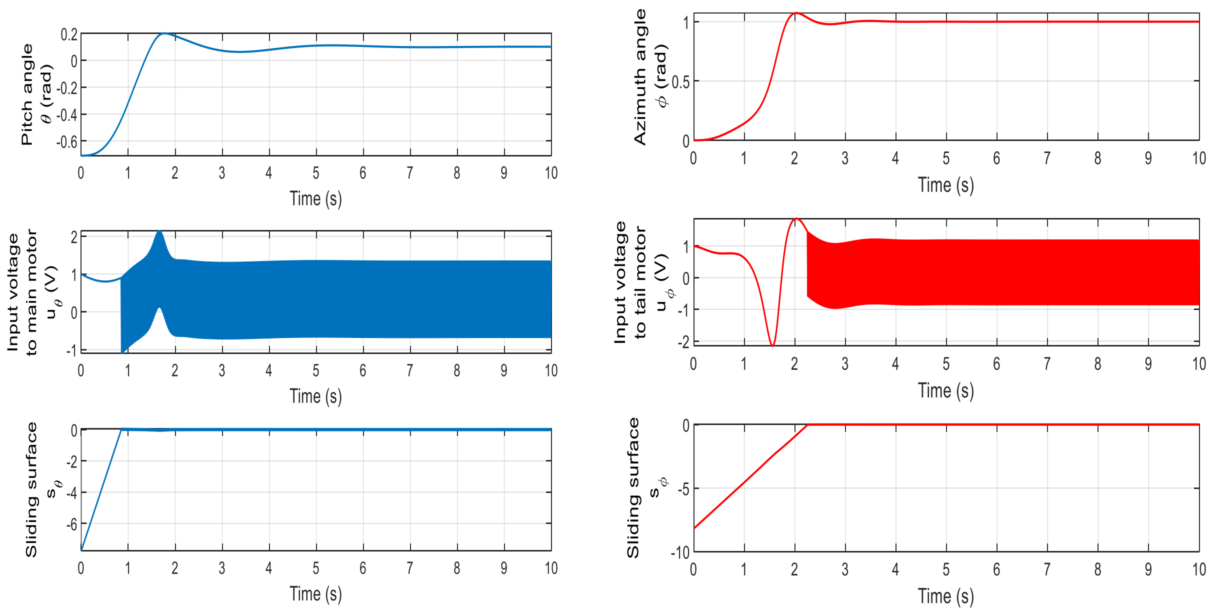

(a) (b)

Figure 2. Step response of the TRAS with the SMC-4 system with IAE (objective function) and GWO (optimization algorithm). Where (a) depicts the Pitch angle, the voltage applied to the main motor, and the vertical sliding surface. and (b) depicts the Azimuth angle, the voltage applied to the tail motor, and the horizontal sliding surface.

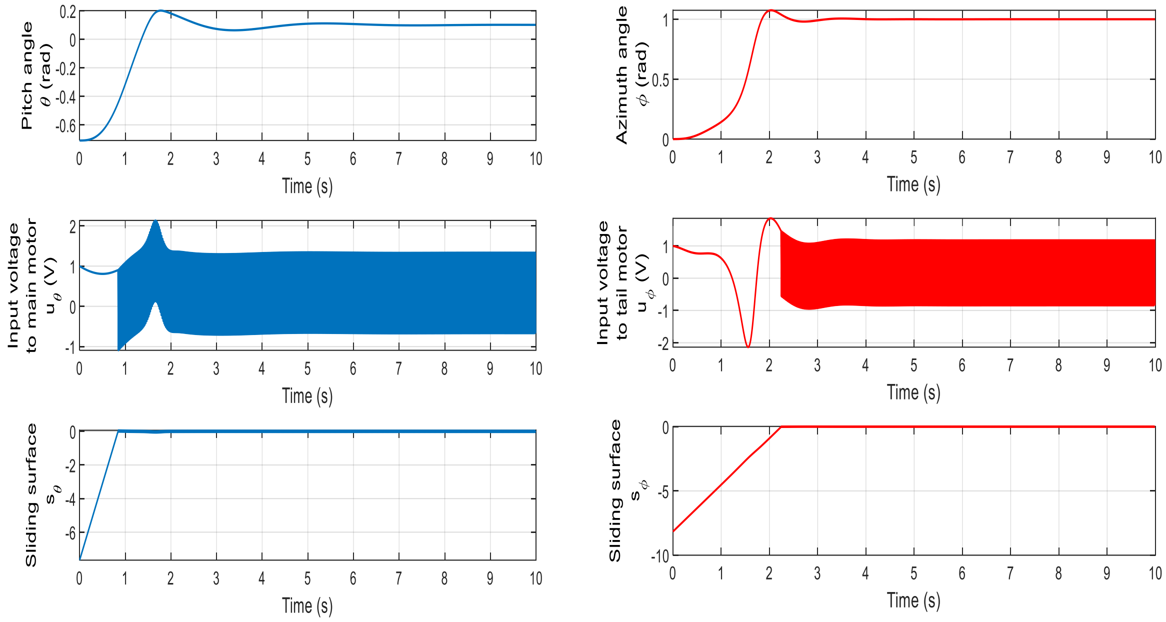

(a) (b)

Figure 3. Step response of the TRAS with the SMC-4 system with IAE (objective function) and WOA (optimization algorithm). Where (a) depicts the Pitch angle, the voltage applied to the main motor, and the vertical sliding surface. and (b) depicts the Azimuth angle, the voltage applied to the tail motor, and the horizontal sliding surface.

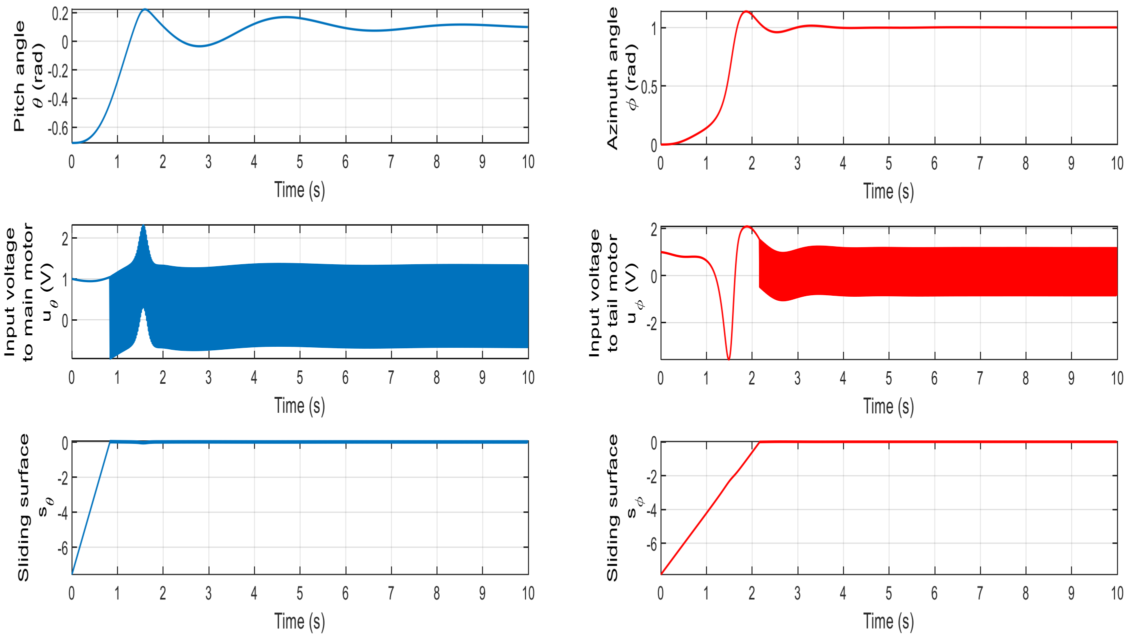

(a) (b)

Figure 4. Step response of the TRAS with the SMC-4 system with ISE (objective function) and GWO (optimization algorithm). Where (a) depicts the Pitch angle, the voltage applied to the main motor, and the vertical sliding surface. and (b) depicts the Azimuth angle, the voltage applied to the tail motor, and the horizontal sliding surface.

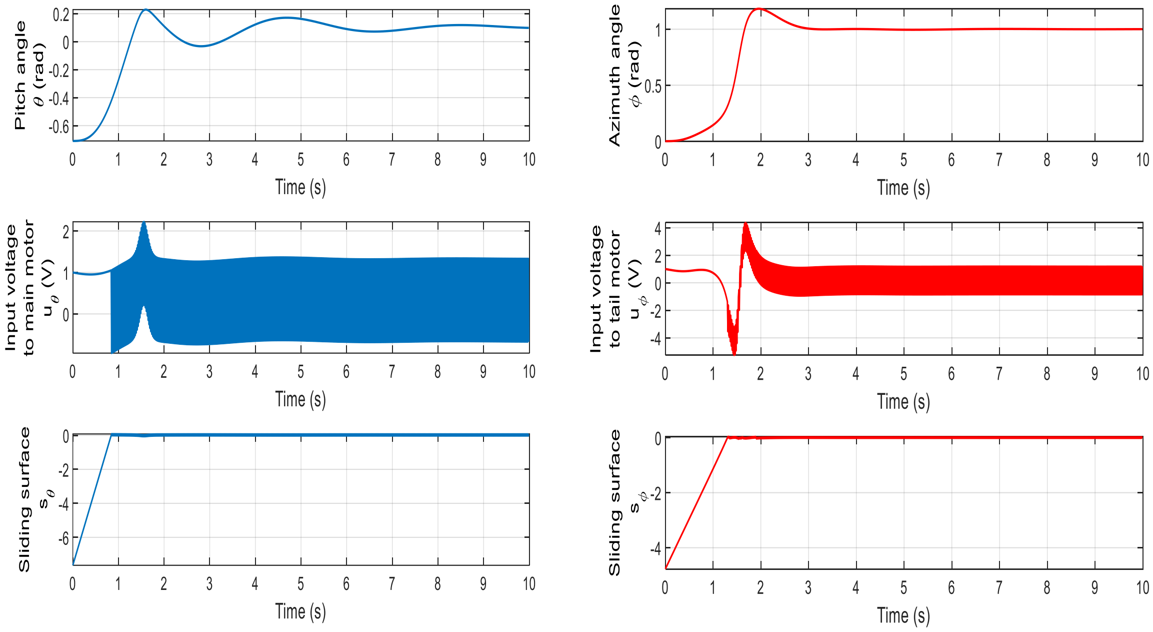

(a) (b)

Figure 5. Step response of the TRAS with the SMC-4 system with ISE (objective function) and WOA (optimization algorithm). Where (a) depicts the Pitch angle, the voltage applied to the main motor, and the vertical sliding surface. and (b) depicts the Azimuth angle, the voltage applied to the tail motor, and the horizontal sliding surface.

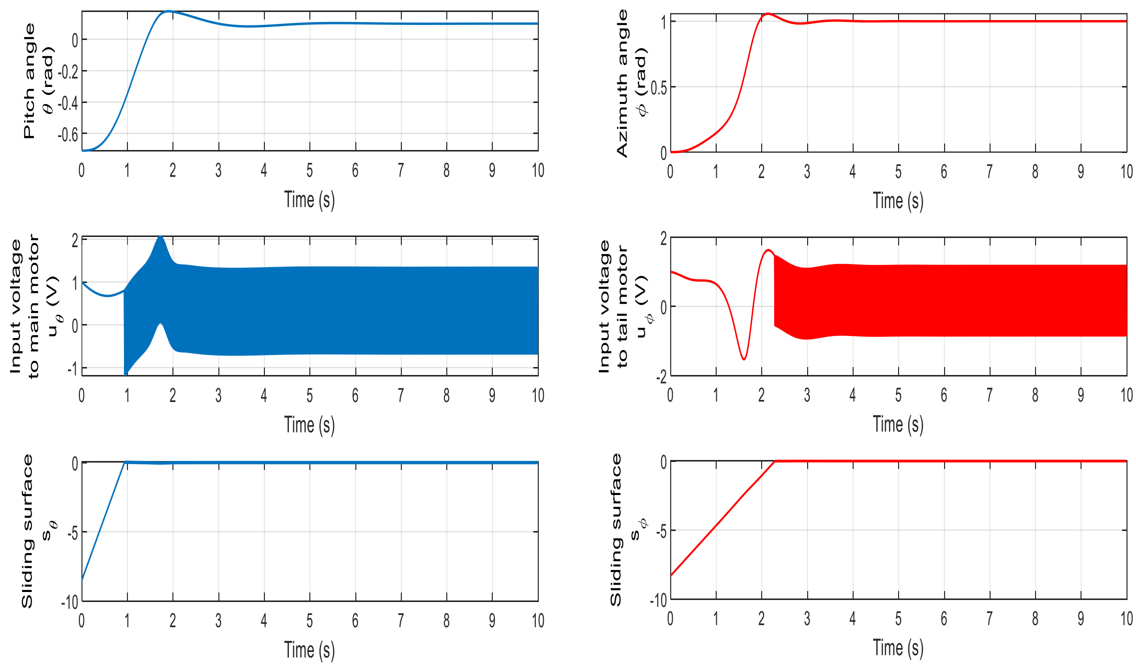

(a) (b)

Figure 6. Step response of the TRAS with the SMC-4 system with ITAE (objective function) and GWO (optimization algorithm). Where (a) depicts the Pitch angle, the voltage applied to the main motor, and the vertical sliding surface. and (b) depicts the Azimuth angle, the voltage applied to the tail motor, and the horizontal sliding surface.

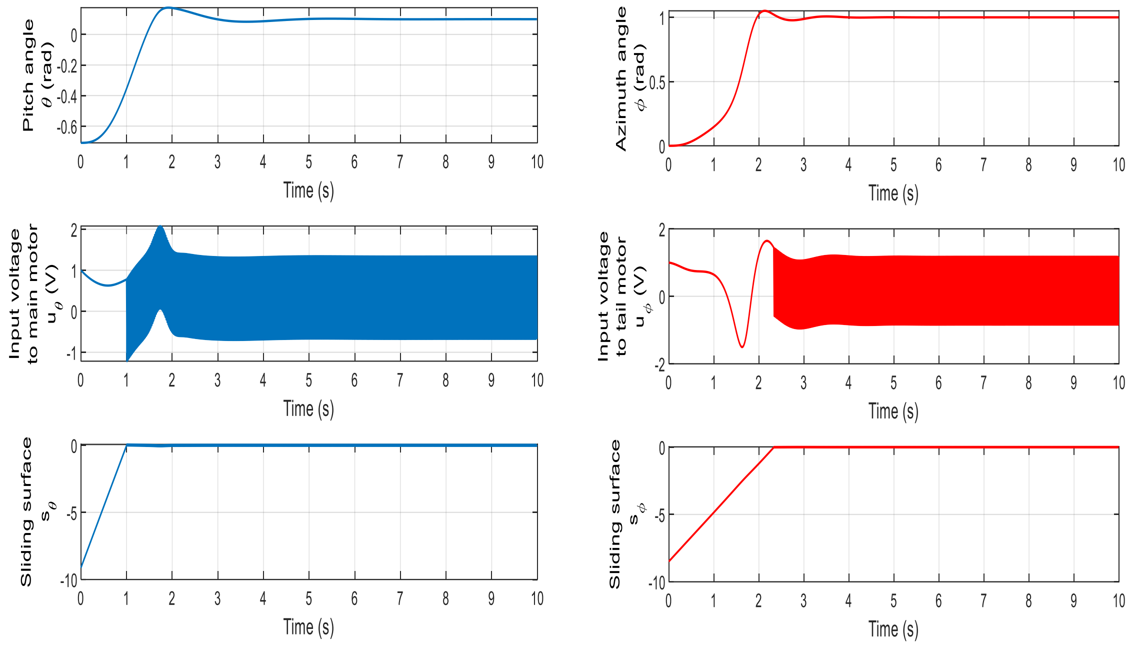

(a) (b)

Figure 7. Step response of the TRAS with the SMC-4 system with ITAE (objective function) and WOA (optimization algorithm). Where (a) depicts the Pitch angle, the voltage applied to the main motor, and the vertical sliding surface. and (b) depicts the Azimuth angle, the voltage applied to the tail motor, and the horizontal sliding surface.

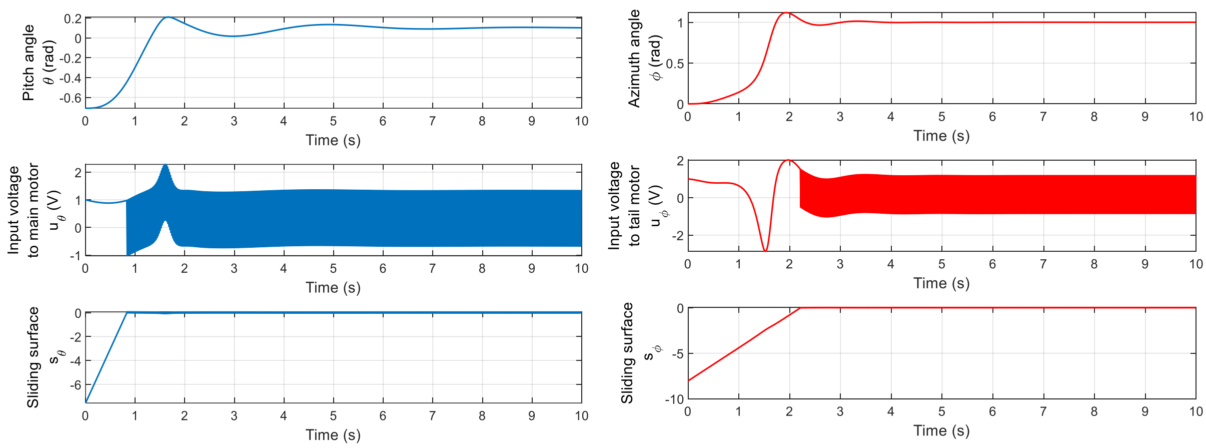

(a) (b)

Figure 8. Step response of the TRAS with the SMC-4 system with ITSE (objective function) and GWO (optimization algorithm). Where (a) depicts the Pitch angle, the voltage applied to the main motor, and the vertical sliding surface. and (b) depicts the Azimuth angle, the voltage applied to the tail motor, and the horizontal sliding surface.

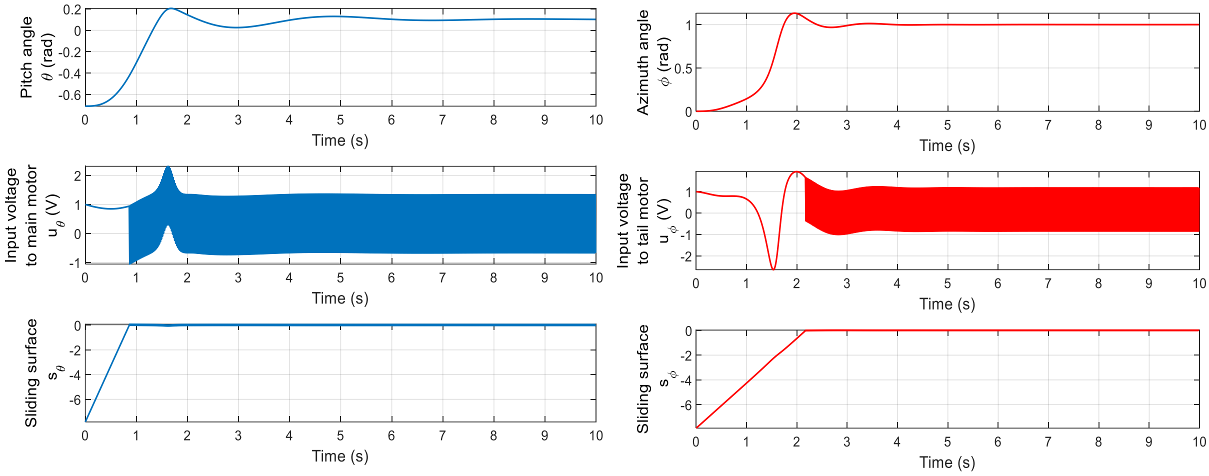

(a) (b)

Figure 9. Step response of the TRAS with the SMC-4 system with ITSE (objective function) and WOA (optimization algorithm). Where (a) depicts the Pitch angle, the voltage applied to the main motor, and the vertical sliding surface. and (b) depicts the Azimuth angle, the voltage applied to the tail motor, and the horizontal sliding surface.

Table 4. System specifications of the SMC-4 system with IAE (objective function).

Transient response specification	GWO		WOA	
	ϕ	**θ**	**ϕ**	**θ**
Rise time	0.92	0.84	0.92	0.84
Settling time	2.78	7.76	2.33	7.85
Delay time	1.52	1.02	1.52	1.02
Percentage overshoot	7.34	100.74	7.49	100.6
Time to reach the sliding surface	2.25	0.85	2.24	0.84
Amplitude of chattering	2.37	3.23	2.39	3.23
ISE	0.88		0.89	
IAE	1.19		1.19	
ITSE	0.53		0.53	
ITAE	0.99		0.99	

Table 5. System specifications of the SMC-4 system with ISE (objective function).

Transient response specification	GWO		WOA	
	ϕ	**θ**	**ϕ**	**θ**
Rise time	0.78	0.77	0.77	0.76
Settling time	2.80	9.71	2.82	9.68
Delay time	1.45	0.98	1.44	0.98
Percentage overshoot	13.83	122.13	18.27	128.85
Time to reach the sliding surface	2.16	0.83	1.31	0.84
Amplitude of chattering	2.55	3.26	9.61	3.16
ISE	0.86		0.86	
IAE	1.26		1.28	
ITSE	0.53		0.53	
ITAE	1.44		1.50	

Table 6. System specifications of the SMC-4 system with ITAE (objective function).

Transient response specification	GWO		WOA	
	ϕ	θ	ϕ	θ
Rise time	1.01	0.90	1.03	0.92
Settling time	2.41	6.22	2.87	6.00
Delay time	1.56	1.05	1.57	1.07
Percentage overshoot	5.74	78.85	5.06	75.33
Time to reach the sliding surface	2.28	0.93	2.33	1.00
Amplitude of chattering	2.38	3.26	2.37	3.29
ISE	0.90		0.90	
IAE	1.20		1.20	
ITSE	0.55		0.56	
ITAE	0.95		0.95	

Table 7. System specifications of the SMC-4 system with ITSE (objective function).

Transient response specification	GWO		WOA	
	ϕ	θ	ϕ	θ
Rise time	0.84	0.81	0.85	0.81
Settling time	2.83	9.89	2.90	9.94
Delay time	1.48	1.00	1.49	1.00
Percentage overshoot	11.98	109.6	13.24	104.5
Time to reach the sliding surface	2.21	0.83	0.86	2.17
Amplitude of chattering	2.52	3.30	2.638	3.36
ISE	0.86		0.86	
IAE	1.21		1.21	
ITSE	0.52		0.52	
ITAE	1.15		1.13	

Therefore, another simulation for a closed loop system was carried out with a simulation time of 10 s. This is apparent in (**Figs. 10-12**). The simulation was based on the design vectors in **Table 3.** which are the optimal parameters of the proposed performance index (IQTAE).

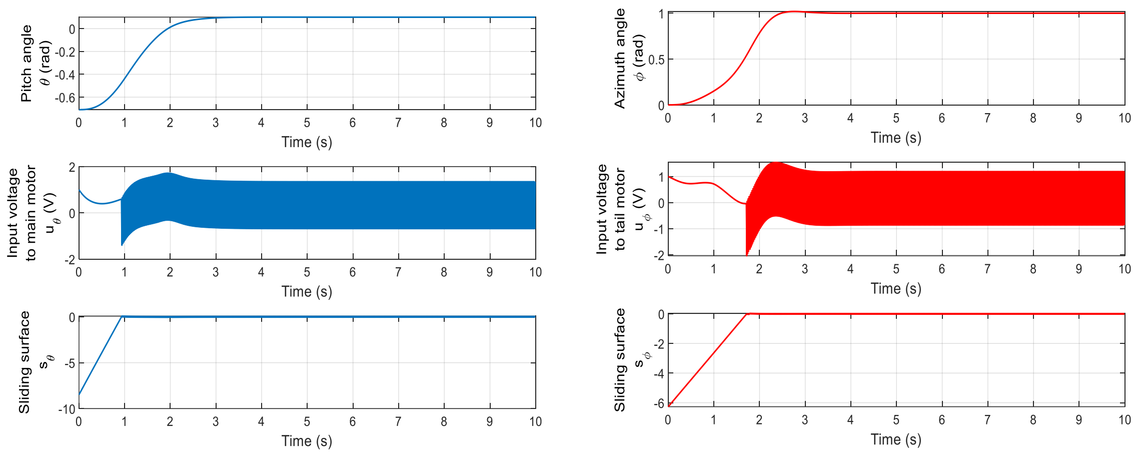

(a) (b)

Figure 10. Step response of the TRAS with the SMC-4 system with IQTAE (objective function) and GA (optimization algorithm). Where (a) depicts the Pitch angle, the voltage applied to the main motor, and the vertical sliding surface. and (b) depicts the Azimuth angle, the voltage applied to the tail motor, and the horizontal sliding surface.

To ensure fairness in the comparison, the same simulation time used in the previous study **(Faisal and Abdulwahhab, 2021c)** is used. The comparison of the transient response specifications of the proposed performance index (IQTAE) with the minimum values of the specifications obtained by the previous study is shown in **Table 8**. The IQTAE enhances the performance of the controller by reducing the overshoot compared to the previous study. The percentage enhancement of the percentage overshoot of both angles reaches 58.7% and 99.35% with GA, -0.65% and 70.1% with PSO, and 44.53% and 88.59% with SA.

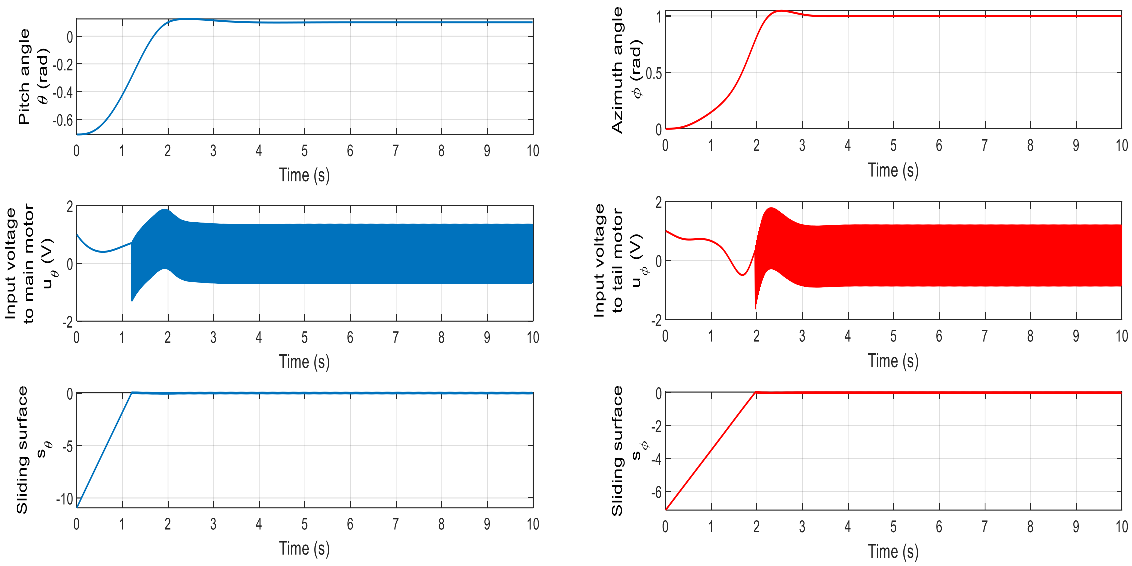

(a) (b)

Figure 11. Step response of the TRAS with the SMC-4 system with IQTAE (objective function) and PSO (optimization algorithm). Where (a) depicts the Pitch angle, the voltage applied to the main motor, and the vertical sliding surface. and (b) depicts the Azimuth angle, the voltage applied to the tail motor, and the horizontal sliding surface.

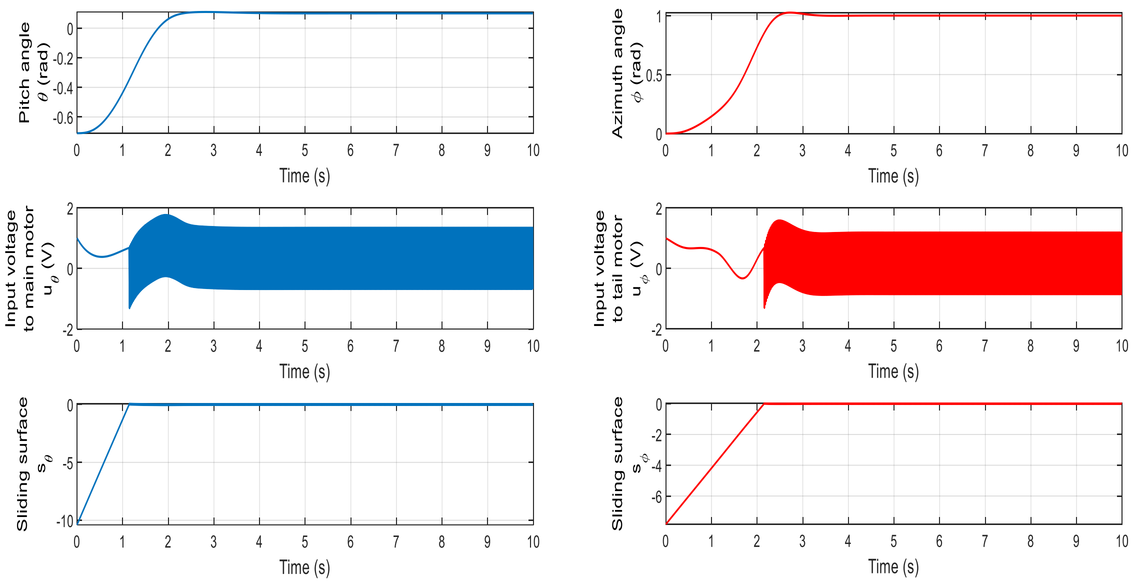

(a) (b)

Figure 12. Step response of the TRAS with the SMC-4 system with IQTAE (objective function) and SA (optimization algorithm). Where (a) depicts the Pitch angle, the voltage applied to the main motor, and the vertical sliding surface. and (b) depicts the Azimuth angle, the voltage applied to the tail motor, and the horizontal sliding surface.

Table 8. Percentage enhancement of system performance using IQTAE compared with **(Faisal and Abdulwahhab, 2021c)**

Transient-Response Specification	GA		PSO		SA	
	ϕ	θ	ϕ	θ	ϕ	θ
Rise time%	-74.3	87	-62.82	-49.35	-79.49	-62.33
Settling time%	-1.27	50	-24.25	40.43	-23.83	35.35
Delay time%	-15.17	-25.5	-15.86	-21.43	-19.31	-24.49
Percentage Overshoot%	58.7	99.35	-0.65	70.18	44.53	88.59
Time to reach the sliding surface%	20.74	-10.71	9.68	-42.86	0.92	-35.71
Amplitude of Chattering%	-50.43	3.41	-46.12	2.48	-24.57	4.64

7. CONCLUSIONS

In this paper, a sliding mode controller is introduced to control the TRAS system and achieve some required specifications. The parameters of this controller were optimized using modern meta-heuristic algorithms, which are a grey wolf optimization algorithm and a whale optimization algorithm. The proposed SMC-4 enhances the overshoot of the system. This was observed by enhancing the IQTAE performance index's value. However, the proposed controller has a chattering issue, which is a common drawback in SMC. As a future work, methods such as implementing a low-pass filter (LPF) or using a high-order SMC can mitigate this issue.

NOMENCLATURE

Symbol	Description	Symbol	Description
θ	The angle from the main rotor (pitch).	F_t	The Propulsive force of the tail rotor.
ϕ	The angles from the tail rotor (azimuth).	ω_m	The angular velocities of the main rotor.
θ_r	Reference pitch angle of TRAS	ω_t	The angular velocities of the tail rotor.
ϕ_r	Reference azimuth angle of TRAS	g_m	The main rotor's DC gain.
J_θ	The sums of moments of inertia relative to the vertical plane	g_t	The tail rotor's DC gain.
J_ϕ	The sums of moments of inertia relative to the horizontal plane	T_m	The main rotor's time constant.
k_1	The first coefficient with respect to the horizontal plane.	T_t	The tail rotor's time constant.
k_2	The second coefficient with respect to the horizontal plane.	g	The acceleration due to gravity.
k_θ	The torque restoration coefficient in the vertical plane.	e_θ	'he error between the reference pitch ngle $\theta_r(t)$ and its actual value $\theta(t)$.
k_ϕ	The torque restoration coefficient in the horizontal plane.	e_ϕ	The error between the reference azimuth angle $\phi_r(t)$ and its actual value $\phi(t)$.
l_{cw}	The length of a counterweight rod with a point mass attached to the end of it.	c_θ	The vertical plane's velocity-proportiona friction torque coefficient.
l_m	The main portion of the beam's length.	c_ϕ	The horizontal plane's velocity-proportional friction torque coefficient.
l_t	The tail portion of the beam's length.	S	The sliding surfaces.
m_{cw}	The Point masses connected to the ends of the counterweight rods.	u_m	The input voltage that is applied to the main DC motor.

m_m	The main propeller's mass.	u_t	The input voltage that is applied to the tail DC motor.
m_t	The tail propeller's mass.	u_{sw}	The switching control in sliding mode controller (SMC).
F_m	The Propulsive force of the main rotor.	u_{t_eq}	The equivalent control in sliding mode controller (SMC).
		sgn	The Sign functions.

Credit Authorship Contribution Statement

Marwa Rasheed Ali: Writing – original draft, Software, Methodology.
Omer Waleed Abdulwahhab: Writing – review & editing, Software, Validation.

Declaration of Competing Interest

The authors declare that they have no known competing financial interests or personal relationships that could have appeared to influence the work reported in this paper.

REFERENCES

Abdulwahhab, O.W. and Abbas, N.H., 2017. A new method to tune a fractional-order PID controller for a twin rotor aerodynamic system. *Arabian Journal for Science and Engineering*, *42*, pp.5179-5189. https://doi.org/10.1007/s13369-017-2629-5

Abdulwahhab, O.W. and Abbas, N.H., 2020. Survey study of factional order controllers. *Journal of Engineering*, *26*(4), pp.188-201. https://doi.org/10.31026/j.eng.2020.04.13

Allouani, F., Boukhetala, D. and Boudjema, F., 2012, March. Particle swarm optimization based fuzzy sliding mode controller for the twin rotor MIMO system. In *2012 16th IEEE Mediterranean Electrotechnical Conference* (pp. 1063-1066). IEEE. https://doi.org/10.1109/MELCON.2012.6196611

Almtireen, N., Elmoaqet, H. and Ryalat, M., 2018. Linearized modelling and control for a twin rotor system. *Automatic Control and Computer Sciences, 52, pp.539-551.* https://doi.org/10.3103/S0146411618060020

Apkarian, P., Bompart, V. and Noll, D., 2007. Non-smooth structured control design with application to PID loop-shaping of a process. *International Journal of Robust and Nonlinear Control: IFAC-Affiliated Journal*, *17*(14), pp.1320-1342. https://doi.org/10.1002/rnc.1175

Bayrak, A., Dogan, F., Tatlicioglu, E. and Ozdemirel, B., 2015. Design of an experimental twin-rotor multi-input multi-output system. *Computer Applications in Engineering Education*, *23*(4), pp.578-586. https://doi.org/10.1002/cae.21628

Borase, R.P., Maghade, D.K., Sondkar, S.Y. and Pawar, S.N., 2021. A review of PID control, tuning methods and applications. *International Journal of Dynamics and Control*, *9*, pp.818-827. https://doi.org/10.1007/s40435-020-00665-4

Butt, S.S. and Aschemann, H., 2015. Multi-variable integral sliding mode control of a two degrees of freedom helicopter. *IFAC-Papers OnLine*, *48*(1), pp.802-807. https://doi.org/10.1016/j.ifacol.2015.05.129

Chen, H., Bowels, S., Zhang, B. and Fuhlbrigge, T., 2019. Controller parameter optimization for complex industrial system with uncertainties. *Measurement and Control*, *52*(7-8), pp.888-895. https://doi.org/10.1177/0020294019830108

Faris, F., Moussaoui, A., Djamel, B. and Mohammed, T., 2017. Design and real-time implementation of a decentralized sliding mode controller for twin rotor multi-input multi-output system. *Proceedings of the Institution of Mechanical Engineers, Part I: Journal of Systems and Control Engineering*, *231*(1), pp.3-13. https://doi.org/10.1177/0959651816680457

Faisal, R.F. and Abdulwahhab, O.W., 2021. Design of a PID-lead compensator for a twin rotor aerodynamic system (TRAS). *Journal of Engineering*, *27*(1), pp.79-88. https://doi.org/10.31026/j.eng.2021.01.06

Faisal, R.F. and Abdulwahhab, O.W., 2021. Design of an adaptive linear quadratic regulator for a twin rotor aerodynamic system. *Journal of Control, Automation and Electrical Systems*, *32*, pp.404-415. https://doi.org/10.1007/s40313-020-00682-w

Faisal, R.F., 2021. Design and Stability Analysis of Twin Rotor Aerodynamic Control Systems. M.Sc. thesis, Department of Electronics and Communication, Computer Engineering, University of Baghdad, Iraq.

Gao, Z.M. and Zhao, J., 2019. An improved grey wolf optimization algorithm with variable weights. *Computational intelligence and neuroscience*, *2019*(1), p.2981282. https://doi.org/10.1155/2019/2981282

Hamoudi, A.K., 2016. Design and simulation of sliding mode fuzzy controller for nonlinear system. *Journal of Engineering*, *22*(3), pp.66-76. https://doi.org/10.31026/j.eng.2016.03.05

Jagadeb, S.R., Subudhi, B. and Naskar, A.K., 2021. Robust two-degree of freedom H∞ control design for a twin rotor multi-input multi-output system with external disturbances and model uncertainties. *Proceedings of the Institution of Mechanical Engineers, Part I: Journal of Systems and Control Engineering*, *235*(5), pp.579-592. https://doi.org/10.1177/0959651820954969

Juang, J.G., Liu, W.K. and Lin, R.W., 2011. A hybrid intelligent controller for a twin rotor MIMO system and its hardware implementation. *ISA transactions*, *50*(4), pp.609-619.https://doi.org/10.1016/j.isatra.2011.06.006

Kumar, M. and Hote, Y.V., 2021. Real-time performance analysis of PIDD2 controller for nonlinear twin rotor TITO aerodynamical system. *Journal of Intelligent and Robotic Systems*, *101*, pp.1-16. https://doi.org/10.1007/s10846-021-01322-4

Liu, C.S., Chen, L.R., Ting, C.S., Hwang, J.C. and Wu, S.L., 2011. Improved twin rotor MIMO system tracking and transient response using fuzzy control technology. *Journal of Aeronautics, Astronautics and Aviation. Series A*, *43*(1), pp.37-43. http://dx.doi.org/10.6125/JoAAA.201103_43(1).05

M Ahmed, E.S. and Mohamed, M., 2009. PID controller tuning scheme for twin rotor multi-input multi-output system based particle swarm optimization approach. *Journal of Engineering Sciences*, *37*(4), pp.955-967. https://dx.doi.org/10.21608/jesaun.2009.127764

Mihaly, V., Şuşcă, M. and Dulf, E.H., 2021. μ-Synthesis FO-PID for twin rotor aerodynamic system. *Mathematics*, *9*(19), p.2504. https://doi.org/10.3390/math9192504

MirJalili, S. and Lewis, A., 2016. The whale optimization algorithm. *Advances in engineering software*, *95*, pp.51-67. https://doi.org/10.1016/j.advengsoft.2016.01.008

Mirjalili, S., Mirjalili, S.M. and Lewis, A., 2014. Grey wolf optimizer. *Advances in engineering software*, *69*, pp.46-61 https://doi.org/10.1016/j.advengsoft.2013.12.007

Mishra, C., Swain, S.K., Mishra, S.K. and Yadav, S.K., 2019, May. Fractional order sliding mode controller for the twin rotor MIMO system. In *2019 International Conference on Intelligent Computing and Control Systems (ICCS)* (pp. 662-667). IEEE. https://doi.org/10.1109/ICCS45141.2019.9065331

Pandey, S.K. and Laxmi, V., 2014, March. Control of twin rotor MIMO system using PID controller with derivative filter coefficient. In *2014 IEEE Students' Conference on Electrical, Electronics and Computer Science* (pp. 1-6). IEEE. https://doi.org/10.1109/SCEECS.2014.6804451

Palepogu, K.R. and Mahapatra, S., 2024. Design of sliding mode control with state varying gains for a Benchmark Twin Rotor MIMO System in Horizontal Motion. *European Journal of Control*, *75*, p.100909. https://doi.org/10.1016/j.ejcon.2023.100909

Paul, P.K. and Jacob, J., 2020. H2 Vs H∞ control of TRMS via output error optimization augmenting sensor and control singularities. *Ain Shams Engineering Journal*, *11*(1), pp.77-85. https://doi.org/10.1016/j.asej.2019.07.001

Rahideh, A., Shaheed, M.H. and Huijberts, H.J.C., 2008. Dynamic modelling of a TRMS using analytical and empirical approaches. *Control Engineering Practice*, *16*(3), pp.241-259. https://doi.org/10.1016/j.conengprac.2007.04.008

Raj, K., Choudhary, S.K. and Muthukumar, V., 2020. Robust finite-time sliding mode control of twin rotor MIMO system. *International Journal of Modelling, Identification and Control*, *35*(1), pp.1-8. https://doi.org/10.1504/IJMIC.2020.113292

Rashad, R., El-Badawy, A. and Aboudonia, A., 2017. Sliding mode disturbance observer-based control of a twin rotor MIMO system. *ISA transactions*, *69*, pp.166-174. https://doi.org/10.1016/j.isatra.2017.04.013.

Roman, R.C., Precup, R.E. and David, R.C., 2018. Second order intelligent proportional-integral fuzzy control of twin rotor aerodynamic systems. *Procedia computer science*, *139*, pp.372-380. https://doi.org/10.1016/j.procs.2018.10.277

Tee, K.P., Ge, S.S. and Tay, F.E., 2008. Adaptive neural network control for helicopters in vertical flight. *IEEE Transactions on Control Systems Technology*, *16*(4), pp.753-762. https://doi.org/10.1109/TCST.2007.912242.

Tao, C.W., Taur, J.S., Chang, Y.H. and Chang, C.W., 2010. A novel fuzzy-sliding and fuzzy-integral-sliding controller for the twin-rotor multi-input–multi-output system. *IEEE Transactions on Fuzzy Systems*, *18*(5), pp.893-905. https://doi.org/10.1109/TFUZZ.2010.2051447

Wen, P. and Lu, T.W., 2008. Decoupling control of a twin rotor MIMO system using robust deadbeat control technique. *IET Control theory and applications*, *2*(11), pp.999-1007. https://doi.org/10.1049/iet-cta:20070335.

Wen, P. and Li, Y., 2011. Twin rotor system modeling, de-coupling and optimal control. In *2011 IEEE International Conference on Mechatronics and Automation* (pp. 1839-1842). IEEE. https://doi.org/10.1109/ICMA.2011.5986259

تصميم وحدة تحكم الوضع المنزلق الامثل لنظام ديناميكي هوائي مزدوج الدوار

مروة رشيد علي*، عمر وليد عبد الوهاب

قسم هندسة الحاسبات، كلية الهندسة، جامعة بغداد، بغداد، العراق

الخلاصة

في هذا البحث تم تقديم نموذج متعدد المدخلات والمخرجات والاقتران العالي غير الخطي للنظام الديناميكي الهوائي ذو الدوار المزدوج (TRAS). يتم اشتقاق النموذج الرياضي للدوار المزدوج باستخدام معادلات لاغرانج. تم تصميم وحدة التحكم في وضع الانزلاق الأمثل (Optimal SMC) لتتبع المسارات المطلوبة بدقة لكل من الزوايا الرئيسية والذيلية. لتصميم معاملات SMC، يتم استخدام خمسة مؤشرات أداء كدوال هدف (objective function). يتم استخدام خوارزميتين للتحسين، وهما خوارزمية الذئب الرمادي (GWO) وخوارزمية الحوت (WOA) لضبط معاملات SMC. ومع ذلك، في العديد من التطبيقات، يكون لل (overshoot) عواقب سلبية مثل الأضرار الميكانيكية وعدم الاستقرار، لذلك، تم اقتراح مؤشر أداء جديد، تم تحديده بواسطة تكامل الاس الرابع للوقت مضروب في مطلق الخطأ (IQTAE) وكانت خوارزمية التحسين المستخدمة مع مؤشر الأداء الجديد هي الخوارزمية الجينية(GA) ، وخوارزمية حركة الجزيئات (PSO) Particleswarm، وخوارزمية التلدين simulannealbnd (SA). يوضح مؤشر الأداء الجديد هذا أن التجاوز(overshoot) قد تم تحسينه – في معظم الحالات – لكل من زاويتي الرأس والذيل. تصل النسبة المئوية للتحسينات في زوايا الرأس والذيل على التوالي إلى 58.7% و99.35% باستخدام خوارزمية GA، و−0.65% و70.1 % باستخدام خوارزمية PSO، و44.53 % و88.59% باستخدام خوارزمية SA .

الكلمات المفتاحية: النظام الديناميكي الهوائي ثنائي الدوار، المسيطر الانزلاقي، مميزات استجابة التردد.